The Plant Cell, Vol. 16, 3341–3356, December 2004, www.plantcell.org © 2004 American Society of Plant Biologists

Translational Regulation via 5′ mRNA Leader Sequences Revealed by Mutational Analysis of the Arabidopsis Translation Initiation Factor Subunit eIF3h

Tae-Houn Kim,[a] Byung-Hoon Kim,[a] Avital Yahalom,[b] Daniel A. Chamovitz,[b] and Albrecht G. von Arnim[a,1]

[a] Department of Botany, University of Tennessee, Knoxville, Tennessee 37996-1100
[b] Department of Plant Sciences, Tel Aviv University, Tel Aviv 69978, Israel

Eukaryotic translation initiation factor 3 (eIF3) consists of core subunits that are conserved from yeast to man as well as less conserved, noncore, subunits with potential regulatory roles. Whereas core subunits tend to be indispensable for cell growth, the roles of the noncore subunits remain poorly understood. We addressed the hypothesis that eIF3 noncore subunits have accessory functions that help to regulate translation initiation, by focusing on the *Arabidopsis thaliana* eIF3h subunit. Indeed, eIF3h was not essential for general protein translation. However, results from transient expression assays and polysome fractionation indicated that the translation efficiency of specific 5′ mRNA leader sequences was compromised in an *eif3h* mutant, including the mRNA for the basic domain leucine zipper (bZip) transcription factor ATB2/AtbZip11, translation of which is regulated by sucrose. Among other pleiotropic developmental defects, the *eif3h* mutant required exogenous sugar to transit from seedling to vegetative development, but it was hypersensitive to elevated levels of exogenous sugars. The ATB2 mRNA was rendered sensitive to the eIF3h level by a series of upstream open reading frames. Moreover, eIF3h could physically interact with subunits of the COP9 signalosome, a protein complex implicated primarily in the regulation of protein ubiquitination, supporting a direct biochemical connection between translation initiation and protein turnover. Together, these data implicate eIF3 in mRNA-associated translation initiation events, such as scanning, start codon recognition, or reinitiation and suggest that poor translation initiation of specific mRNAs contributes to the pleiotropic spectrum of phenotypic defects in the *eif3h* mutant.

INTRODUCTION

Developmental phase transitions in plants are exquisitely sensitive to environmental factors. Germination, the transition from embryogenesis to seedling development, is one of several complex transitions that are under environmental control. After the induction of germination, which is partially controlled by light, stress conditions, such as drought, trigger a post-germinative growth arrest that is mediated by the hormone abscisic acid (Lopez-Molina et al., 2001). Subsequently, the decision between two distinct developmental pathways, photomorphogenesis in the light and etiolation in darkness, is under the control of the *CONSTITUTIVE PHOTOMORPHOGENESIS* (*COP*) and DE-ETIOLATED (*DET*) genes, which function as repressors of light signaling in darkness (reviewed in Kim et al., 2002; Wei and Deng, 2003). Six of the *COP*/*DET* genes encode subunits of an octameric protein complex, the COP9 signalosome (CSN) (Chamovitz et al., 1996; Serino et al., 2003). The CSN is required in darkness for the proteolytic turnover of LONG HYPOCOTYL5 (HY5) and HY5-HOMOLOG, two light regulatory transcription factors (Osterlund et al., 2000; Holm et al., 2002), but it also regulates other processes, such as auxin signaling (Schwechheimer et al., 2001). Biochemically, the CSN impinges on protein turnover by promoting the cleavage of a ubiquitin-like peptide, NEDD8, from the cullin subunit of SKP1/cullin/F-box protein class E3 ubiquitin ligases (Lyapina et al., 2001; Schwechheimer et al., 2001). However, the spectrum of biochemical activities of the CSN continues to be refined, given that neddylation defects do not correlate precisely with the phenotypic severity of *csn* mutants (Mundt et al., 2002; Wang et al., 2003b). Additional roles for the CSN have been proposed in the phosphorylation of signaling molecules, such as p53 and c-Jun (Bech-Otschir et al., 2001; Uhle et al., 2003), and in the deubiquitination of SKP1/cullin/F-box protein complex subunits (Zhou et al., 2003).

The CSN is structurally and evolutionarily related to two other multisubunit protein complexes, the proteasome lid subcomplex and eukaryotic translation initiation factor 3 (eIF3; Asano et al., 1997b; Hofmann and Bucher, 1998; Kim et al., 2001). Subunits of these three so-called PCI complexes contain one of two conserved amino acid motifs, the PCI domain (proteasome/COP9/Int6), which may play a role in complex assembly, or the MPN domain (Mpr1-Pad1-N terminus), which can play a catalytic role (Cope et al., 2002; Maytal-Kivity et al., 2002; Verma et al., 2002). Biochemical interactions exist between the CSN and eIF3 across the eukaryotic kingdom (Hoareau-Alves et al., 2002; Wee et al., 2002; Maytal-Kivity et al., 2003). Interest in this

[1] To whom correspondence should be addressed. E-mail vonarnim@utk.edu; fax 865-974-0978.
The author responsible for distribution of materials integral to the findings presented in this article in accordance with the policy described in the Instructions for Authors (www.plantcell.org) is: Albrecht G. von Arnim (vonarnim@utk.edu).
Article, publication date, and citation information can be found at www.plantcell.org/cgi/doi/10.1105/tpc.104.026880.

area was galvanized by the finding that eIF3 subunits c and e copurify with the CSN in plants (Karniol et al., 1998; Yahalom et al., 2001).

The functional significance of interactions between eIF3 and other PCI complexes remains to be defined, for it may hold clues to a fundamental cross talk between translation and protein turnover processes in the eukaryotic cell. A key discovery was that the fission yeast eIF3e/Int6 subunit not only binds to the proteasome lid but also stimulates proteasome activity (Yen and Chang, 2000; Yen et al., 2003). Notwithstanding an emerging structural model for budding yeast eIF3 (Valasek et al., 2002), the roles of most eIF3 subunits remain poorly understood, even in the context of translation. EIF3 stimulates charging of the 40S small ribosomal subunit with the ternary complex, composed of eIF2, GTP, and $tRNA^{Met}$ as well as recruitment of the resulting 43S complex to the mRNA via the cap binding complex eIF4F (Hershey and Merrick, 2000). Wheat (*Triticum aestivum*) and *Arabidopsis thaliana* eIF3 were purified as 11-subunit protein complexes (Burks et al., 2001). EIF3 subunits accumulate asynchronously during seed development and heat shock (Gallie et al., 1998), suggesting that eIF3 is a dynamic and heterogeneous complex. Only five eIF3 subunits, a, b, c, g, and i, are considered core subunits because they are highly conserved and essential for protein translation in yeast (Asano et al., 1998; Hershey and Merrick, 2000; Koyanagi-Katsuta et al., 2002). Whereas some of the remaining, noncore, eIF3 subunits may still support basal translation, others may play stabilizing or regulatory roles (Bandyopadhyay et al., 2000, 2002; Crane et al., 2000; Guo et al., 2000; Matsumoto et al., 2002). Specifically, misregulation of the noncore subunits eIF3e and eIF3h may predispose mammalian cells to tumorous growth (Rasmussen et al., 2001; Saramaki et al., 2001; Mayeur and Hershey, 2002). The ensuing hypothesis that specific noncore subunits directly regulate the translation of specific cellular mRNAs remains to be tested experimentally.

As a step toward elucidating the potential functions of noncore eIF3 subunits and the role of interactions between eIF3 and the CSN, we investigated the CSN-associated eIF3h protein, presenting a loss-of-function mutation for a noncore eIF3 subunit in a multicellular organism. Our results suggest that eIF3h is dispensable for general protein translation in Arabidopsis, but rather regulates the translation of a subset of mRNA transcripts through their 5′ leader sequences. Among the pleiotropic developmental phenotypes of *eif3h* mutants, some can be understood by our dovetailing molecular and physiological data, which suggest that eIF3h underlies a translational regulatory mechanism in response to external sugars.

RESULTS

A Hypomorphic Allele of eIF3h Shows Pleiotropic Growth Defects throughout Development

We previously reported that the CSN complex from cauliflower (*Brassica oleracea*) copurifies with a small number of extraneous proteins and among these, two subunits of eIF3, eIF3e and eIF3c. A third copurifying protein, originally referred to as a MOV34 protein (Karniol et al., 1998), corresponds to the recently identified 40-kD h subunit of eIF3 in Arabidopsis (At1g10840.1; Burks et al., 2001). Arabidopsis eIF3h is encoded by a single gene, and similar sequences encode human eIF3h and a putative eIF3h subunit in fission yeast (Figure 1). The apparent absence of eIF3h in budding yeast has defined eIF3h as a noncore subunit and suggested that eIF3h, along with eIF3e and certain other eIF3 subunits, may perform a regulatory or accessory role in eIF3 (Asano et al., 1997a, 1997b; Bandyopadhyay et al., 2002).

To investigate the role of eIF3h in Arabidopsis, we isolated a recessive mutant allele (*eif3h*-1) carrying a T-DNA insertion in the 10th exon (Figure 2A). A truncated eIF3h-related protein was detected in this allele (Figure 2B). Homozygous *eif3h-1* mutant plants displayed postembryonic growth retardation (Figures 2C and 3A). Vegetative shoot and root growth, flowering, and senescence were delayed compared with the wild type. Phenotypic rescue of the *eif3h*-1 mutant was accomplished with a transgene harboring a fusion of the *eIF3h* promoter and coding region (Figures 2D and 2E), thus confirming that the mutant phenotypes observed were a result of the disruption of the *eIF3h* gene. Approximately 80% of *eif3h-1* mutant plants arrested their development as vegetative rosettes (Figure 3A) and died, regardless of whether the plants were grown in soil or on sterile medium. In the remaining plants, shoot axillary meristems often became activated late in the growth period, leading to a bushy appearance characteristic of a loss of apical dominance (Figure 3B). After germination in darkness, hypocotyl length was reduced and seedlings displayed an open hook and separation of the cotyledons (Figure 3C), features characteristic of a defect in etiolation. A second *eIF3h* insertion allele carrying a T-DNA in the eleventh intron (e*if3h-2*) had a similar phenotype as *eif3h-1* (Figure 2C). An eIF3h protein truncated by ~2 kD accumulated in the *eif3h-2* mutant (Figure 2B). Morphological phenotypes of the *eif3h-1* mutant, such as bushiness, epinastic cotyledons, warped leaves, poor gravitropism, occasional pin-formed inflorescence bolts, and a short primary root with few root hairs (Figures 2C and 3F; data not shown), suggested an altered auxin response. Consistent with this notion, the mRNA levels of two auxin-inducible genes were elevated slightly in the absence (*IAA3* and *IAA14*) or the presence (*IAA3*) of added auxin, whereas the level of *IAA17* remained normal (Figure 3G). The selfed *eif3h-1* mutant flowers typically harbored only four or five stamens instead of the usual six, a small fraction of which lacked fully developed anthers (Figure 3D). Seedset in the club-like siliques (Figure 2D) was greatly reduced (Figure 3E, Table 1). Although the number of seed per fruit increased upon cross-pollination of *eif3h-1* with wild-type pollen (data not shown), cross-pollination did not completely rescue the runty appearance of the progeny seeds (Table 2), suggesting that the fertility defect in the *eif3h-1* mutant is in part maternal. In addition, the *eif3h-1* mutant male gametophyte competed poorly against the wild type (Table 2). However, no such defect was observed for the female gametophyte (Table 2), in turn suggesting that the maternal effect is a sporophytic one. Transmission of the *eif3h-2* allele was similarly impeded, as judged on the basis of the segregation of the *eif3h-2* phenotype and the inserted kanamycin resistance gene (Table 2).

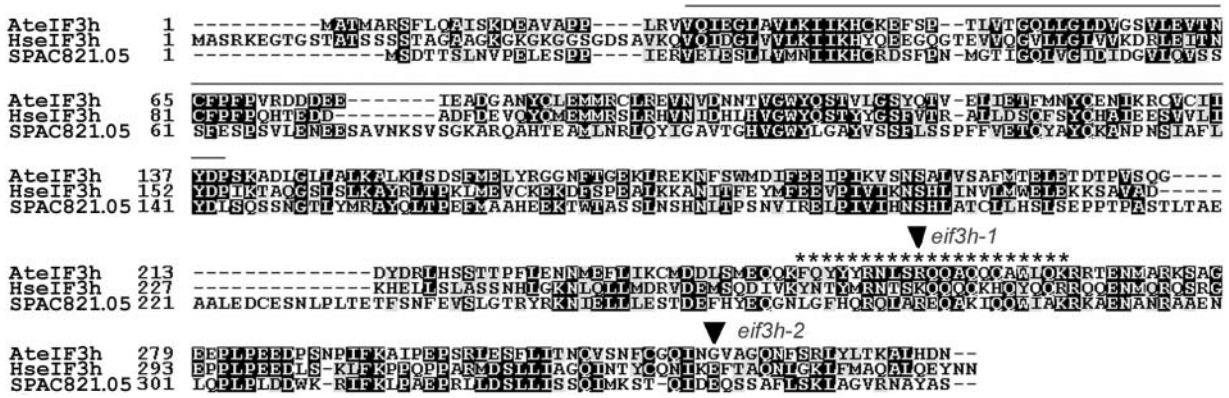

Figure 1. Sequence Comparison of the eIF3h Protein.

Comparison between eIF3h protein sequences of Arabidopsis (At; At1g10840.1), human (Hs; AAC84044), and a putative fission yeast homolog (Sp; CAB57439.1, 26% identity). The peptide sequence that identified eIF3h as copurifying with the CSN (Karniol et al., 1998) is indicated with asterisks. The MPN domain is marked by a line, and the insertion sites of two T-DNA alleles in the corresponding DNA sequence are indicated by arrowheads.

eIF3h Protein Is Widely Expressed but Is Not Required for Stability of Other eIF3 Subunits

The eIF3h protein accumulated in all organs tested yet was most abundant in roots and flowers (Figure 4A). In the CSN, as is often the case for multimeric complexes, loss of any one subunit results in the destabilization of the entire complex and some of its constituent subunits (Chamovitz et al., 1996; Wei and Deng, 1999). By contrast, upon loss of eIF3h, the rest of the eIF3 complex remained structurally coherent as judged by gel filtration and immunodetection of the eIF3b core subunit (Figure 4B), although the apparent molecular weight of eIF3 was reduced in the *eif3h-1* mutant. In addition, the protein level of at least two core subunits, eIF3b and eIF3c, and one noncore subunit, eIF3e, remained stable in the *eif3h-1* mutant (Figure 4C). Although eIF3h could associate with the CSN (Karniol et al., 1998), loss of eIF3h did not affect accumulation of its CSN4 or CSN5 subunits (Figure 4C). Vice versa, no difference was detected in the level of two eIF3 subunits, eIF3b and eIF3h, in *csn1* or *csn7* mutants (Figure 4D). Therefore, the CSN does not seem to control the stability of these eIF3 subunits.

The *eIF3h* Gene Is Necessary for Normal Sugar and Hormone Responses

The *eif3h-1* mutant showed a biphasic response to external sugars. In the absence of sucrose in the medium, *eif3h-1* mutant seedlings arrested their development before primary leaf expansion (Figure 5A, left column). By contrast, 1% sucrose prevented the developmental arrest, indicating that *eif3h-1* needs an exogenous sugar source after germination. However, 1% sucrose also delayed the greening process (Figure 5A, second column). Similar results were obtained with maltose and glucose, but not with the nonhydrolyzable but osmotically active sugar mannitol (Figure 5B; data not shown). Furthermore, at or above 2% sucrose, full germination of *eif3h-1* was inhibited (Figure 5C), and purple anthocyanin pigments persisted in the hypocotyl (Figure 5A, third column). Inhibition of greening, induction of anthocyanins, and a block in post-germinative seedling development are sugar signaling responses that can be seen with 6% sucrose in wild-type Arabidopsis (Figure 5A, right column; Rook and Bevan, 2003). These results indicate that the sugar signaling pathway is hypersensitized in the *eif3h-1* mutant. As in many Arabidopsis mutants (Leon and Sheen, 2003; Rook and Bevan, 2003), *eif3h-1*'s sensitivity to sugars during early germination was accompanied by elevated sensitivity to abscisic acid (ABA; Figures 5D and 5E).

Synergistic Genetic Interaction between *eif3h-1* and a *csn* Mutant

Partial rescue of root growth by 1% sucrose, inhibition of germination by 6% sucrose, and sucrose-dependent anthocyanin accumulation were also observed in the *csn1*/*fus6* mutant (Figure 6C; Castle and Meinke, 1994). Although the postembryonic growth arrest of the *csn* mutant was certainly not fully rescued by external sucrose, these results illustrate a limited phenotypic overlap between *eif3h* and *csn* mutants, consistent with a functional relationship between the eIF3 and CSN protein complexes.

To confirm that eIF3h is a true component of eIF3 in Arabidopsis and to examine the potential for interactions between Arabidopsis eIF3h and the CSN, yeast two-hybrid and coimmunoprecipitation assays were employed (Figures 6A and 6B). Yeast two-hybrid assays revealed the potential for direct physical interactions of eIF3h with full-length eIF3a, eIF3b, and eIF3c, consistent with eIF3h as a component of eIF3. Furthermore, in line with the copurification of eIF3h with the cauliflower CSN (Karniol et al., 1998), eIF3h interacted directly with Arabidopsis CSN1, CSN7, and CSN8 in yeast (Figure 6A) but not with CSN4 or CSN5 (data not shown).

Next, coimmunoprecipitation experiments with wild-type Arabidopsis seedling extracts using an antiserum generated against

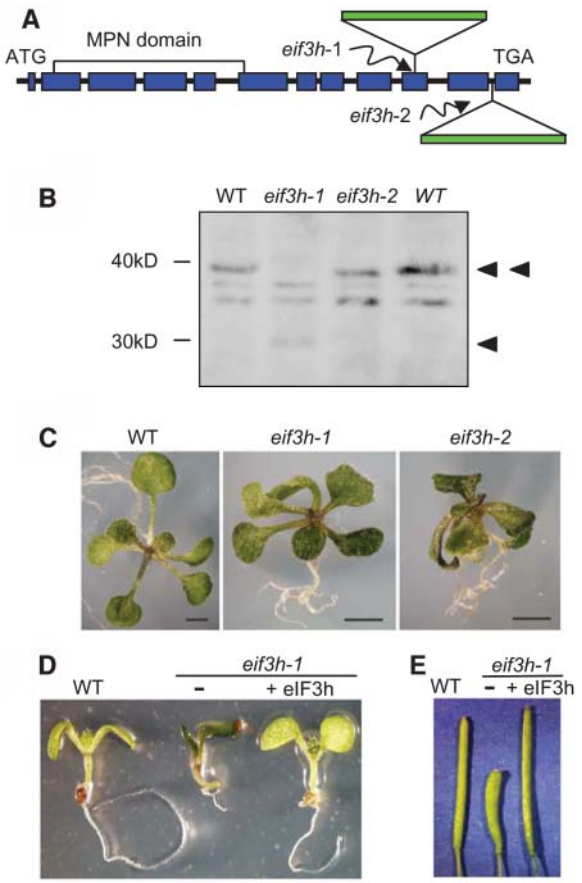

Figure 2. Characterization of *eIF3h* T-DNA Insertion Alleles.

(A) T-DNA integration sites in the *eIF3h* gene. Boxes denote exons, and lines represent introns. The *eif3h-1* allele has a T-DNA in the 10th exon downstream of Ser^{254}, and *eif3h-2* has an insertion downstream of base pair 64 in the 80-bp-long 11th intron. The conserved MPN domain (Mpr1-Pad1-N terminus) is highlighted.

(B) Immunoblot analysis with affinity-purified eIF3h antibody using 15 μg of seedling protein extract demonstrates the accumulation of truncated eIF3h proteins in two mutant alleles. The positions of eIF3h proteins are indicated with arrowheads. Two cross-reacting bands are visible.

(C) Two-week-old seedlings of the wild type, *eif3h-1*, and *eif3h-2* are shown. Bar = 2 mm.

(D) Functional complementation of *eif3h-1*. Comparison of a 7-d-old wild-type seedling (left), the *eif3h-1* mutant (middle), and a transformant with a recombinant *eIF3h* gene in the *eif3h-1* mutant background (right).

(E) Fruit morphology was also rescued by complementation.

eIF3h demonstrated an interaction between eIF3h and two other eIF3 subunits, the core subunit, eIF3b, and the noncore subunit, eIF3e (Figure 6B), confirming that eIF3h is an eIF3 subunit. Complementing the yeast two-hybrid data, we also observed a weak coimmunoprecipitation of eIF3h with the CSN subunits CSN4 and CSN5 (Figure 6B). Taken together, and in light of the negative yeast two-hybrid interaction, these results may suggest that a fraction of eIF3h interacts with the CSN complex. The interaction with CSN4 and CSN5 may be indirect (i.e., mediated by an interaction with CSN1, CSN7, or CSN8).

The genetic interaction between the *CSN* and *eIF3h* was explored with the help of double mutants between *eif3h-1* and the *csn8-1* loss of function mutation. *CSN8* (*COP9*) encodes the smallest subunit of the CSN. The most vigorous double mutant individuals displayed an embryonic growth arrest characterized by a severe retardation of hypocotyl and root growth beginning at the early torpedo stage. However, the cotyledons continued to expand and were able to accumulate anthocyanin as is typical for *csn8* mutants (Figure 6D). No similar embryos were detected among more than 100 embryos from *eif3h* lineages lacking the mutant *csn8* allele. The double mutant families also harbored more severely defective embryos, characterized by morphological arrest at the globular or heart stage, often followed by continued volume growth (data not shown). The mutual enhancement of the *csn8* and *eif3h* phenotypes reveals that eIF3h and the CSN do play important roles in mid-embryogenesis, despite the absence of overt phenotypes in either single mutant, and that the functional relationship is agonistic rather than antagonistic.

eIF3h Is Not Required for General Translation but May Control Translation of Specific mRNAs

Considering that disruption of eIF3h was not lethal and that other subunits of eIF3 remained stable in the absence of the h subunit, we tested whether eIF3h might be dispensable for translation. To this end, *eif3h-1* and wild-type translation products were pulse labeled in vivo with ^{35}S-Met and ^{35}S-Cys followed by SDS-PAGE of equal amounts of proteins and autoradiography (Figure 7A). However, no reduction in the overall incorporation of labeled amino acids was detected in the *eif3h-1* mutant.

Whereas the fission yeast eIF3e/Int6 subunit plays a role in protein ubiquitination (Yen et al., 2003), no difference in overall ubiquitination levels was observed in the Arabidopsis *eif3h-1* mutant (Figure 7B). Together, these results led us to hypothesize that eIF3h plays a regulatory role in translation. To explore this further, we examined whether and how eIF3h might affect the translation of specific mRNAs. Selected 5′ leader sequences were compared for their translational capacity between *eif3h* mutants and the wild type using a dual-luciferase reporter assay (Figure 7C). Individual leaders were inserted upstream of the firefly luciferase (FLUC) start codon and transformed transiently into *eif3h-1* mutant and wild-type seedling leaves together with a reference construct containing a Renilla luciferase (RLUC) gene. Translational efficiency was expressed as the ratio of FLUC and RLUC activity. The 5′ leader of the ATB2 gene, which encodes the basic leucine zipper protein (bZip), AtbZip11, was chosen because of the sugar hypersensitivity of the *eif3h* mutant and because the ATB2 5′ leader contains a sugar-dependent translational inhibitor motif (Rook et al., 1998a; Wiese et al., 2004). Notably, the activity of the FLUC reporter gene fused to the ATB2 leader was reduced fourfold, on average, in the *eif3h-1* mutant compared with the wild type (Figure 7E; $P < 0.001$, Student's *t* test), despite equal mRNA abundance of ATB2:FLUC, TL:RLUC, and endogenous ATB2 controls (Figure 7D). Inhibition of translation was also observed for the leader of the myb protein LATE ELONGATED HYPOCOTYL (LHY) ($P < 0.001$; Schaffer et al., 1998; Kim et al., 2003). Both the ATB2 and LHY leaders also caused underexpression in plants carrying the

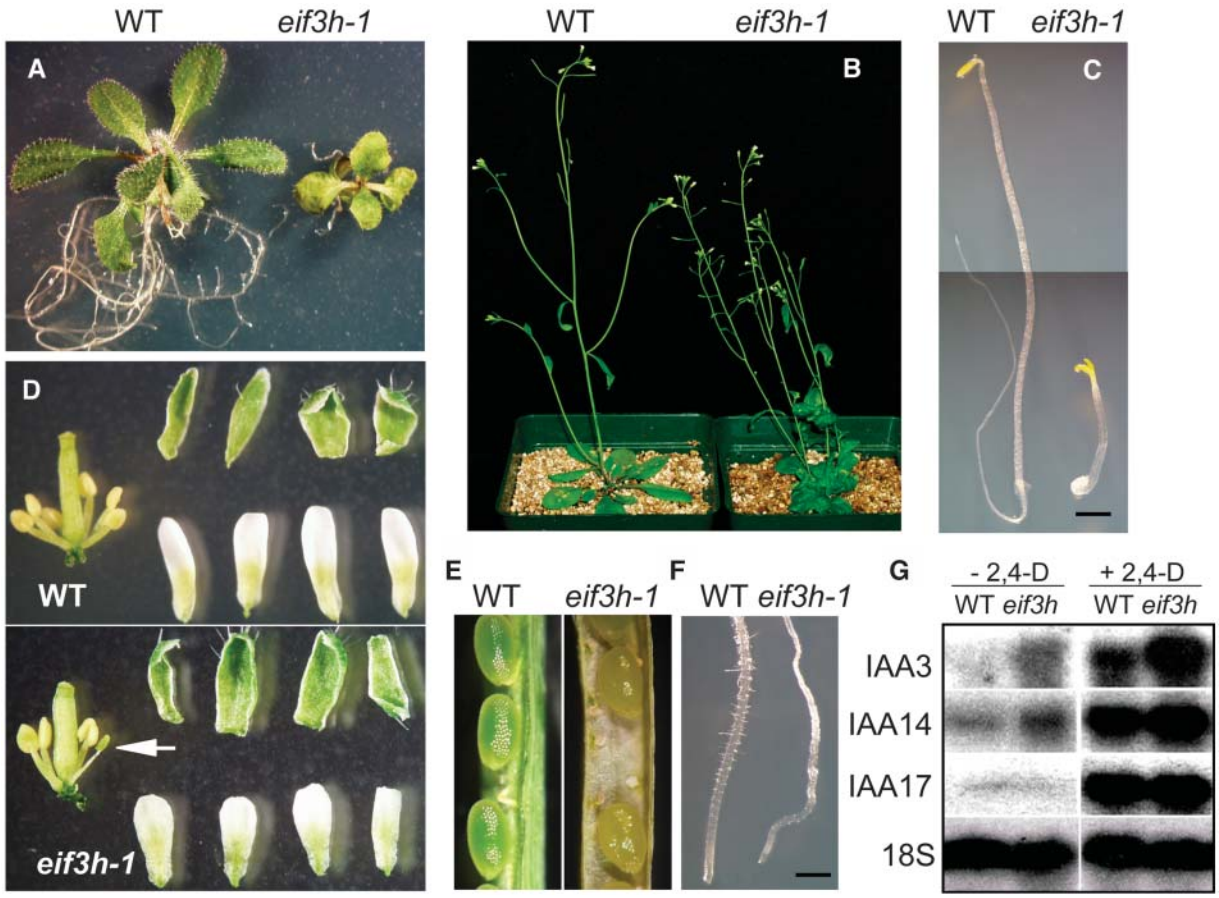

Figure 3. Pleiotropic Developmental Phenotypes of *eif3h-1.*

(A) Twenty-five-day-old plants of the wild type and *eif3h-1*. Note lack of expanding leaves in the apex of the arrested *eif3h-1* mutant.
(B) Surviving adult *eif3h-1* mutant plants have a branched inflorescence and low fertility.
(C) Compared with wild-type seedlings (left), the *eif3h-1* mutant (right) has a short hypocotyl and separated cotyledons when germinated in darkness. Bar = 1 mm.
(D) Flowers of the wild type and *eif3h-1* were dissected to show reduced stamen number; note developmentally defective anther (arrow).
(E) Dissected fruits of the selfed *eif3h-1* mutant reveal partial seed abortion.
(F) Root hair formation is inhibited in *eif3h-1*. Bar = 1 mm.
(G) RNA gel blot hybridization with AUX/IAA gene probes in *eif3h-1* mutants and wild-type seedlings germinated on 1 μM of the auxin 2,4-D for 6 d. Probes were specific for *IAA3* (GenBank accession C00011, At1g04240), *IAA14* (C00046, At4g14550), *IAA17* (At1g04250), and 18S rRNA as a loading control.

eif3h-2 allele (Figure 7F). In contrast with ATB2 and LHY, several other leaders tested drove translation as effectively in *eif3h-1* as in the wild type; these included the leaders of ABSCISIC ACID INSENSITIVE5 (ABI5), the omega (Ω) leader of *Tobacco mosaic virus* (TMV), the small subunit of Rubisco (RBCS), and the bZip protein HY5 (Figure 7G). A moderate, yet significant ($P < 0.05$) difference in expression was observed for chlorophyll *a/b* binding protein 2 (CAB2). The poor translation of the ATB2 leader in the *eif3h-1* mutant was partially rescued by transiently coexpressing eIF3h during the assay (Figure 7E) but not when yellow fluorescent protein (YFP) was included as a negative control instead. These results suggest an immediate, rather than an indirect, effect of eIF3h on translation driven by specific mRNA leader sequences. When expression levels were assayed separately from cotyledons, primary leaves, and upper leaves, the *eif3h-1* mutant showed generally lower ATB2-FLUC levels in each organ (Figure 7H). We also confirmed with the help of a 35S: β-glucuronidase plasmid that the range of cell types transformed using particle bombardment was comparable between the wild type and *eif3h-1* (data not shown).

To seek independent evidence for a role of eIF3h in translation initiation on specific mRNAs, we compared *eif3h-1* mutants and the wild type for the distribution of specific mRNAs in sucrose gradients designed to fractionate polysomal and nonpolysomal RNA, followed by detection of specific transcripts by RT-PCR. No dramatic difference in the UV absorbance profile or rRNA electrophoresis profile was detected (Figure 8), further arguing against a global defect in translation initiation in the *eif3h-1*

Table 1. The Selfed *eif3h* Mutant Shows Reduced Fertility as Well as a Defect in Stamen Development

Phenotype	Wild Type	*eif3h*
Seeds/fruit	54.3 ± 3.2	15.9 ± 7.1
Aborted seeds/fruit	0.2 ± 0.4	21.8 ± 8.3
Stamens/flower	6 ± 0	4.4 ± 0.6
Abnormal stamens/flower	0 ± 0	0.6 ± 0.6

The ± indicates standard deviation ($n = 50$).

mutant. However, a reduction in the polysome loading of the endogenous ATB2 mRNA was detected in the *eif3h-1* mutant (Figure 8D). For comparison, the rbcS mRNA did not significantly change its distribution between polysomal and nonpolysomal fractions. To guard against the possibility that the differences in PCR product accumulation might be attributable to inhibitors of RT-PCR amplification, the RNA fractions were spiked with luciferase RNA as an internal control after fractionation of the gradient. The efficiency of amplification was approximately the same in all fractions (Figure 8E). Using different amounts of template mRNA for amplification, we also confirmed that the reactions shown in Figure 8 had not reached saturation (data not shown).

The ATB2 leader contains five AUG codons in four upstream open reading frames (uORFs; Figure 9A), of which one, uORF2b, represses translation in response to external sucrose (Rook et al., 1998a; Wiese et al., 2004). As a first step toward identifying the sequences that render mRNAs sensitive to the level of eIF3h, several mutant ATB2 leaders were examined in the transient assay. Indeed, a leader lacking uORFs 1, 2a/2b, and 4 was no longer sensitive to the eIF3h level (Figure 9B). Because sensitivity to *eif3h* was only partially abolished by mutation of AUG number 2b (Figure 9B) or 2a (data not shown), it appears that eIF3h helps to overcome the cumulative inhibitory effect on translation that is exerted by multiple uORFs.

In wild-type plants, the translational activity of the ATB2:FLUC reporter was specifically repressed by sucrose (Figure 9C), consistent with previous conclusions (Rook et al., 1998a); for comparison, the HY5 leader was insensitive to sucrose. To test whether the eIF3h protein is directly responsible for the sucrose repression of the ATB2 leader, we shifted plants from 1% sucrose, the concentration optimal for *eif3h* seedling growth, to other sucrose concentrations (Figure 9D). In the wild type, the ATB2 leader was again repressed by sucrose within 48 h. In the *eif3h-1* mutant, the initial slope of the sucrose response curve was less steep (i.e., the response to 0 and 2% sucrose was not significantly different compared with 1%), although 6% sucrose continued to inhibit ATB2 translation approximately threefold, similar to the wild type (Figure 9D). For comparison, the ATB2/1-4 mutant did not show inhibition by sucrose in this assay, as expected. These results suggest that eIF3h is necessary for efficient translation initiation on the wild-type ATB2 mRNA leader, regardless of whether sucrose, in conjunction with the regulatory uORF 2b, is repressing its translation or not.

Taken together, these results indicate that the translation factor eIF3h is critical for high-level protein expression from only a specific subset of mRNAs, such as ATB2 and LHY, rather than for global translation. Therefore, we conclude that the developmental and sugar response phenotypes of the *eif3h* mutant are not caused by a general reduction in translational initiation but are more likely to be the consequence of altered initiation of specific mRNAs, such as the ATB2 and LHY mRNAs.

DISCUSSION

Translational control plays a key role in numerous developmental and physiological processes. In plants, translational regulation contributes to the regulation of specific genes in response to environmental cues, such as water and heat stress, sugar homeostasis, and light–dark transitions, and it also affects viral gene expression (reviewed in Kawaguchi and Bailey-Serres, 2002). Beyond plants, translation initiation is regulated via pathways involving the cap binding protein, eIF4F, as well as via eIF2, the factor responsible for loading $tRNA^{Met}$ onto the 40S ribosomal subunit (Pestova et al., 2001; Hinnebusch and Natarajan, 2002). By comparison, regulatory activities, if any, of the largest initiation factor, eIF3, remain poorly defined. Here, we characterized the developmental and physiological consequences of a deficiency in one subunit of eIF3, eIF3h. The *eif3h-1* mutant described here represents a detailed examination of a germinal mutation in an eIF3 subunit in a multicellular organism. Our data provide strong evidence for a regulatory role for eIF3h because the translation of specific mRNAs was differentially compromised in this mutant. The specificity of *eif3h*'s translational defect was unexpected given that eIF3 is not known to interact directly with standard mRNAs. The *eif3h*-sensitive mRNAs are expected to possess one or more common structural features that render them dependent on a more complete set of translation factors, perhaps in conjunction with other mRNA binding proteins. Moreover, we extended the data on the biochemical interaction between eIF3

Table 2. Transmission of *eif3h* Alleles

		Progeny Phenotypes[a]			
Parents		Morphology		Kanamycin Resistance[b]	
Female	Male	eif3h /Total	(%)	Kan^r /Total	(%)
Maternal Effect		Seed Morphology			
eif3h-1 (−/−)	*eif3h-1* (−/−)	95/171	55.5		
eif3h-1 (−/−)	Wild type	41/92[c]	44.5		
Wild type	*eif3h-1* (−/−)	0/70	0.0		
eif3h-1 (+/−)	*eif3h-1* (+/−)	0/89	0.0		
Gametophytic Transmission		Seedling Morphology			
eif3h-1 (+/−)	Wild type	0/155	0.0	73/155	47.1
Wild type	*eif3h-1* (+/−)	0/116	0.0	3/116	2.6
eif3h-1 (+/−)	*eif3h-1* (+/−)	57/586	9.7	381/683	55.8
eif3h-2 (+/−)	*eif3h-2* (+/−)	72/667	10.8	328/478	68.6

[a] Experiments were repeated three times with similar results.
[b] Transmission of the *eif3h* T-DNA alleles was scored via the linked kanamycin resistance (Kan^r).
[c] Mature seeds of *eif3h* (−/−) plants tend to be small and deformed compared with the wild type.

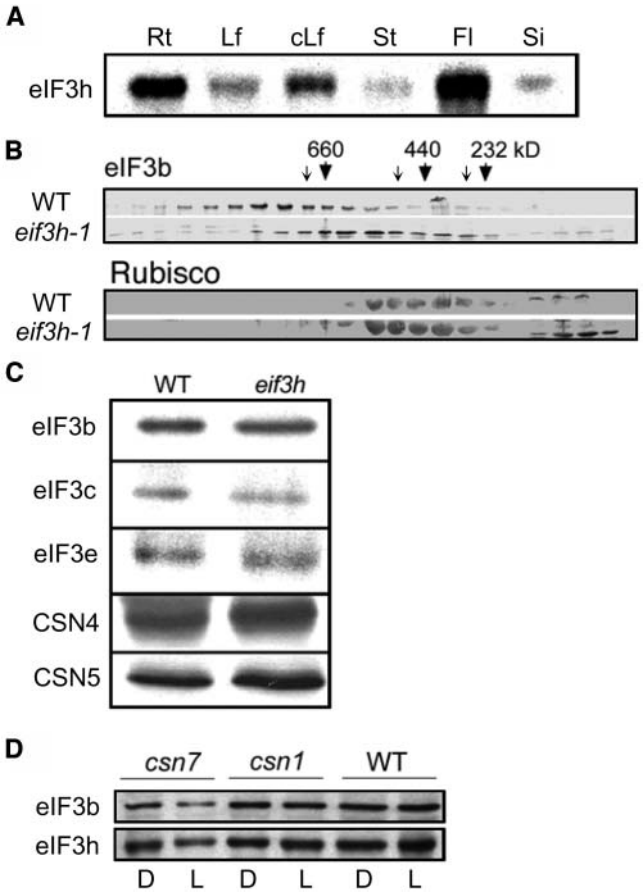

Figure 4. Protein Expression Studies.

(A) Immunoblot analysis of eIF3h protein accumulation with protein extracts from roots (Rt), rosette leaves (Lf), cauline leaves (cLf), stems (St), flowers (Fl), and siliques (Si). Equal amounts (20 μg) of protein were loaded per lane.

(B) Gel filtration chromatography (Superose 6HR, Pharmacia) of light-grown wild type and *eif3h-1* mutant protein extracts. Fractions containing eIF3 were revealed by immunoblotting using antibodies against eIF3b. Peak fractions of molecular mass markers are indicated. As a control, the mobility of the ribulose-1,5-bisphosphate carboxylase/oxygenase (Rubisco) enzyme complex, which can be detected because of cross-reactivity of the eIF3b antiserum, remained unchanged.

(C) Immunoblots of total protein extracts from wild-type and *eif3h-1* mutant seedlings probed with antibodies against eIF3b, eIF3c, eIF3e, CSN4, and CSN5.

(D) Protein gel blot analysis of eIF3b and eIF3h protein levels in seedling extracts from the wild type and the indicated *csn* mutants grown in darkness (D) or white light (L) for 6 d.

subunits and the CSN complex, which may represent a pathway for the coordination of translation initiation and protein turnover.

eIF3h May Function as a Translational Regulator

Translational regulation often involves specific RNA binding proteins that recognize sequence elements in the 5′ leader or 3′ untranslated region (Dean et al., 2002). Typically, these proteins communicate with the translation initiation machinery via the eIF4 cap binding complex. Regulatory roles of eIF3 are less well established, yet not entirely unprecedented. Apart from this work, little evidence for an mRNA-specific role in translation has been provided for eIF3 or any of its subunits. A viral transactivator of ribosome shunting interacts with eIF3 (Park et al., 2001, 2004). Moreover, the mammalian eIF3e subunit has been implicated in regulating translation from viral RNAs (Hui et al., 2003; Wang et al., 2003a). EIF3e/Int6 is the target of an antiviral defense pathway orchestrated by the interferon-inducible P56 protein, which specifically inhibits the interaction of eIF3 with the ternary complex (Guo et al., 2000; Hui et al., 2003). This and perhaps other effects of P56 differentially affect the translation of cap-dependent mRNAs and of polycistronic RNAs containing internal ribosome entry sites (Hui et al., 2003; Wang et al., 2003a). More recently, a temperature-sensitive point mutation of the budding yeast eIF3 core subunit, eIF3b/PRT1, has shown defects in translation initiation of the uORF containing GCN4 leader, implicating eIF3 in processes downstream of 48S complex assembly, such as resumption of scanning by the 40S ribosome or in start codon selection (Nielsen et al., 2004). These findings have set a precedent for the concept that mutations in the general translation factor eIF3 can differentially affect distinct species of mRNA. However, the Arabidopsis *eif3h* mutation differs from the *prt1* mutation in one major respect, namely, that the polysome profile is dramatically altered in *prt1* but not in *eif3h* mutants. Therefore, the *eif3h* mutation appears to have a more subtle effect.

Translational Role of eIF3h

Concerning Arabidopsis eIF3h, coimmunoprecipitation and yeast two-hybrid experiments clearly corroborated that eIF3h is an authentic subunit of Arabidopsis eIF3 (Burks et al., 2001), although our data leave open the possibility that eIF3h may exist independent of eIF3, either in association with the CSN or in another form. Mutation of the eIF3h subunit did not cause a major disruption of the eIF3 complex (Figures 4B and 4C), prompting us to directly address the hypothesis that eIF3h may regulate translation in an mRNA-specific fashion. The key finding is that seven 5′ mRNA leader sequences tested were differentially sensitive to the level of eIF3h over a fourfold range (Figure 7). Although the 35S promoter is expected to drive similar levels of FLUC and RLUC mRNA transcription in wild-type and mutant plants, and the transcript levels as estimated by RT-PCR were similar, we cannot categorically exclude that some proportion of the differential luciferase ratios observed may be attributable to differing FLUC or RLUC transcript levels in the mutant versus the wild type, rather than differences in protein translation. It should be noted that the reduced expression of the ATB2 leader in the *eif3h* mutant cannot simply be explained by the developmental retardation of the *eif3h* mutant seedlings because translatability was lower than the wild type in both juvenile and more adult leaves (Figure 7H). The finding that inclusion of an eIF3h expression construct caused partial rescue of ATB2 translation

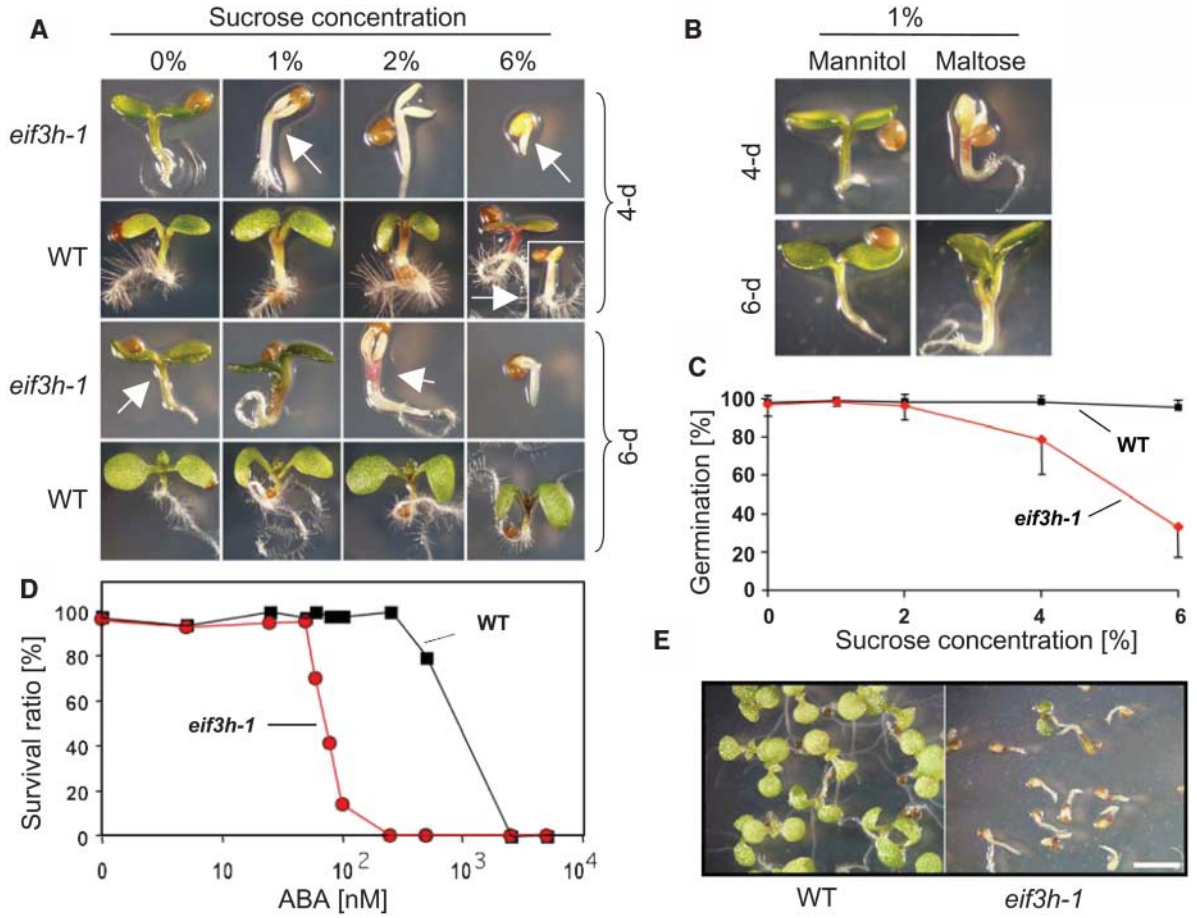

Figure 5. Sucrose and ABA Responses in the *eif3h-1* Mutant.

(A) Seedlings were germinated on increasing concentrations of sucrose for the indicated times. Note the developmental arrest of the *eif3h-1* mutant by day 4 in the absence of sucrose as well as hypersensitivity of *eif3h* to sucrose (arrows). The inset shows that growth arrest begins to occur at 6% sucrose in the wild type.

(B) *eif3h-1* mutant seedlings were germinated on 1% mannitol or maltose for 4 or 6 d.

(C) The germination rate (emergence of radicle from seed coat) of *eif3h-1* (red) decreased with increasing concentrations of sucrose, whereas wild-type seeds germinated efficiently (black). Bars denote standard deviations.

(D) Seedlings of *eif3h-1* (red circles) and the wild type (black squares) were germinated on ABA. Survival of ABA-induced growth arrest (i.e., greening of the cotyledons), was scored after 6 d. Standard deviations were typically smaller than symbols.

(E) Seedlings of *eif3h-1* and the wild type were germinated on 0.1 μM ABA for 6 d. Bar = 5 mm.

(Figure 7E) is consistent with a direct, rather than an indirect, developmental effect of the *eif3h* mutation on translational efficiency.

Is there a common feature that renders mRNA leader sequences sensitive to an *eif3h* mutation? Initial experimental evidence hints at multiple short uORFs, although there may well be other as yet unknown features that sensitized our gene expression cassettes to a mutation in *eIF3h*. Both the ATB2 and LHY leaders contain five upstream AUGs. Meanwhile, the leader sequences of the CAB2 and RBCS mRNAs, which, along with the TMV Ω leader, lack uORFs, were only mildly compromised if at all by the *eif3h* mutation. However, the presence of a uORF alone does not automatically render an mRNA sensitive to the eIF3h level. For example, the HY5 leader contains a single uORF, whereas the ABI5 leader contains a single AUG that is immediately followed by a stop codon, a situation known to depress translation in vitro (Zhang and Maquat, 1997). The site-directed mutants of the ATB2 leader tested provide compelling evidence for the importance of multiple uORFs. Eliminating just one out of five upstream AUGs improved translatability only marginally in the *eif3h* background, even in the case of uORF 2b, which is functionally important for sucrose repression of ATB2 translation (Figure 9B; Wiese et al., 2004). However, once four out of five upstream AUGs were removed, leaving just the five-codon-long uORF3, translatability increased dramatically to a level indistinguishable from the wild type.

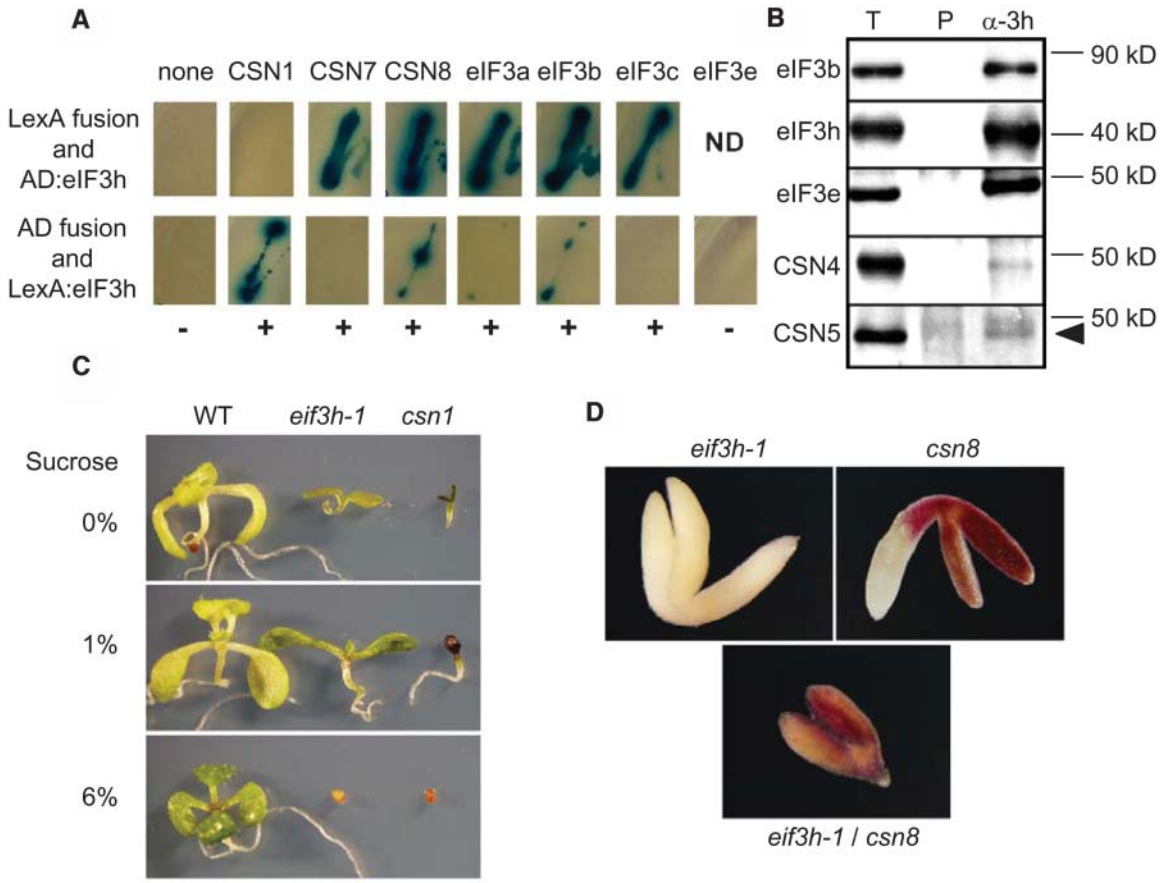

Figure 6. Biochemical and Genetic Interaction between *eif3h-1* and *csn* Mutants.

(A) Yeast two-hybrid assay. Transformed yeast strains harboring the indicated fusions to the LexA DNA binding domain or a transcriptional activation domain (AD) were grown on medium containing X-Gal and lacking Leu to simultaneously check for both β-galactosidase (dark pigment) and *leu2* reporter gene expression. A plus sign below each column indicates a positive interaction in at least one of two combinations. ND, not determined because of autonomous reporter activation by LexA-eIF3e. None of the other LexA fusions yielded autonomous activity (data not shown). Reversing the bait and prey partners is known to occasionally abolish a yeast two-hybrid interaction because of steric constraints.

(B) Coimmunoprecipitates were collected from wild-type Arabidopsis extracts (2 mg of protein) with antiserum against eIF3h (right lane, α-3h) or preimmune serum (middle lane, P). The total protein extract (20 μg of protein) was loaded as a positive control (first lane, T). Protein gel blots were probed with the indicated antisera. Arrowhead indicates CSN5 signal.

(C) Stimulation of anthocyanin accumulation and of root growth at 1% sucrose as well as inhibition of seed germination in response to 6% sucrose were observed in both *eif3h-1* and *csn1* (*fus6-1*) mutants.

(D) Embryos mutant for *eif3h-1* only (left), *csn8* only (right), and *eif3h csn8* double mutants (center) were dissected out from nearly mature seeds. Images were taken at the same magnification.

The uORF 2b in the ATB2 leader is conserved among a subset of bZip mRNAs (Martinez-Garcia et al., 1998) and governs a sucrose-induced repression of translation (Rook et al., 1998a; Wiese et al., 2004). Given that ATB2 remained sucrose sensitive in the *eif3h* mutant (Figure 9D), one might rule out that eIF3h is a direct component of the sucrose-induced repression of translation pathway. There was no variation in abundance of eIF3h protein under different concentrations of sucrose (T.-H. Kim and A.G. von Arnim, unpublished data). However, eIF3h is obviously needed for the efficient expression of the ATB2 leader under low sucrose levels; thus, eIF3h underlies the translational derepression in the absence of sucrose. Assuming yet again that eIF3h is indeed aiding the translational machinery to surmount multiple uORFs, it is plausible that ATB2 uORFs other than 2b continue to be encountered by the translation apparatus in the absence of sucrose, rather than being skipped by a bypass or leaky scanning mechanism.

Thus, the conclusion emerging from these data is that eIF3h may function generally to overcome the inhibitory effect of short uORFs, which are found in many plant transcription factor mRNAs (Lohmer et al., 1993; Martinez-Garcia et al., 1998; Rook et al., 1998a; Wang and Wessler, 1998). What might be the mechanistic role of eIF3h during translation initation? The classical function of eIF3 is to assist in loading of the ternary

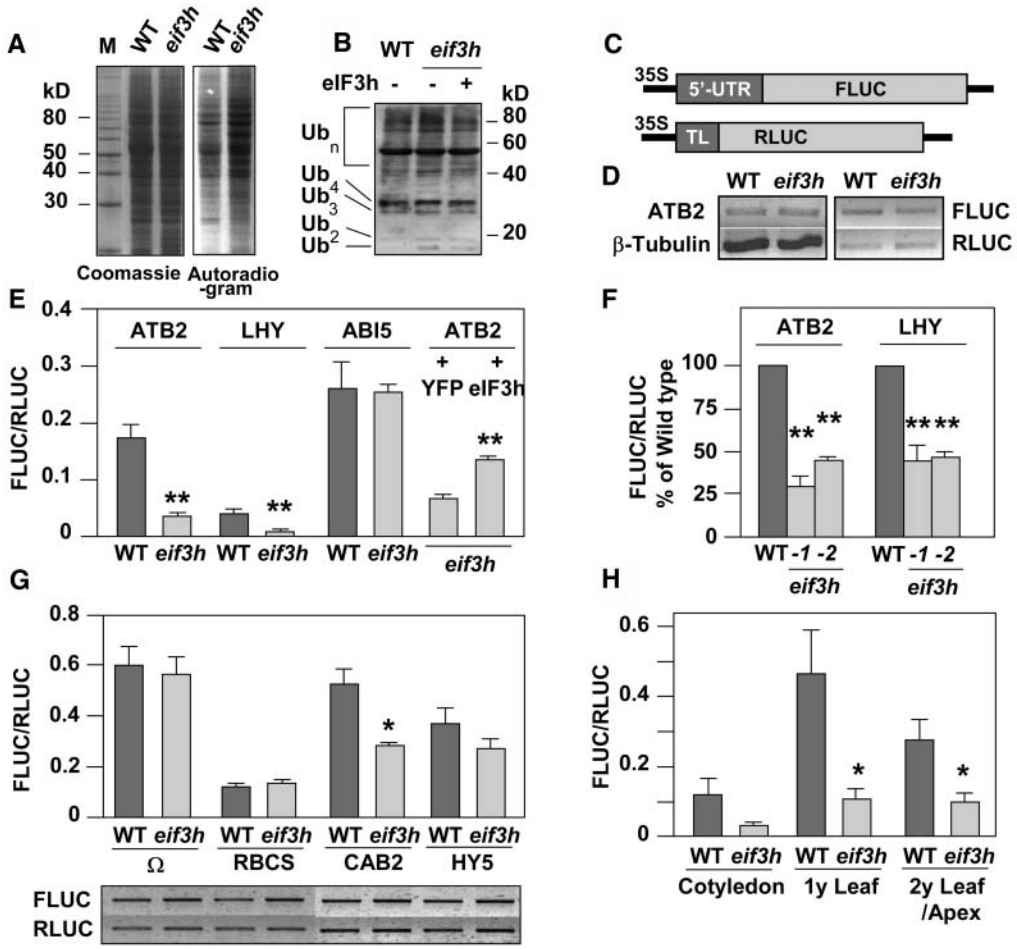

Figure 7. eIF3h Is Implicated in the Translational Efficiency of Specific mRNAs.

(A) The rate of de novo protein synthesis was examined by in vivo labeling of Arabidopsis seedlings with ^{35}S-Met and Cys for 1 h. After radiolabeling, total proteins were extracted and equal amounts were separated by SDS-PAGE. The right panel is the autoradiogram of the Coomassie blue–stained gel on the left.

(B) The level of total ubiquitinated proteins was examined by immunoblot analysis with a polyclonal antibody against ubiquitin. Wild-type seedlings were compared with *eif3h-1* mutant seedlings without (−) or with (*eIF3h*) a complementing *eIF3h* transgene.

(C) Reporter constructs for dual luciferase assays. The FLUC coding region was fused to the 5′ leader (5′-UTR) of the tested genes. RLUC containing the translational leader from tobacco etch virus (TL) served as an internal control in each transient transformation. Both reporters are under the control of a 35S promoter. Leader sequences are described in Methods.

(D) to **(H)** Wild-type and *eif3h* plants grown for 10 d on MS agar plates containing 1% sucrose were cotransfected by particle bombardment. As a control, transiently expressed mRNA transcript levels were compared by RT-PCR. Similar levels of transcripts were detected in the wild type and mutant in all cases. The efficiency of translation was calculated as the ratio of FLUC and RLUC activity from typically three or four independent experiments. Bars denote standard errors. Asterisks symbolize the results from a Student's *t* test in a pairwise comparison, with the control bar directly adjacent to the left. One asterisk, $P < 0.05$; two asterisks, $P < 0.001$.

(D) Transcript levels after transformation of ATB2:FLUC and TL:RLUC were compared by RT-PCR (right panel). PCR products of ATB2 and β-tubulin represent the mRNA expression of the endogenous genes (left panel).

(E) Translation of the ATB2, LHY, and ABI5 5′ leader sequences was tested in leaves of wild-type and *eif3h-1* seedlings. Where indicated, a third plasmid expressing a wild-type eIF3h cDNA (+eIF3h) or YFP as a negative control were cobombarded with the ATB2:FLUC and TL:RLUC plasmids.

(F) Translation of ATB2-FLUC and LHY-FLUC was tested in *eif3h-2* seedlings and contrasted with expression in *eif3h-1* and the wild type. The wild type is set to 100%, and bars represent standard errors.

(G) Translation of reporters containing 5′ leaders of tobacco mosaic virus (Ω), RBCS, CAB2, and HY5 was tested in the *eif3h-1* mutant and the wild type. The bottom panel shows the level of FLUC and RLUC RT-PCR products amplified from corresponding RNA samples.

(H) The ATB2-FLUC and TL-RLUC plasmids were coexpressed as in **(D)**. Extracts were prepared separately from cotyledons, primary leaves, and the remaining upper portion of wild-type or *eif3h-1* seedlings.

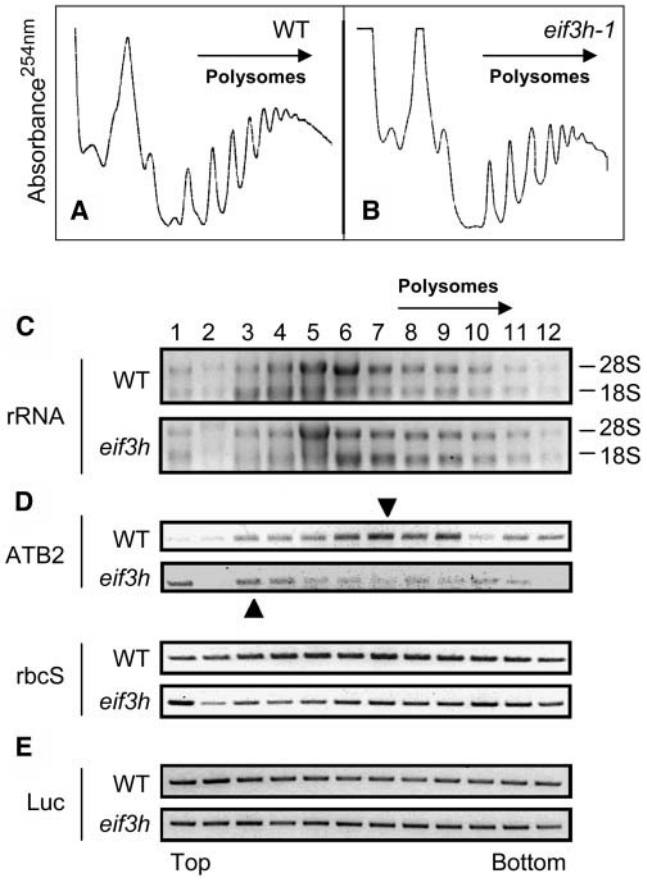

Figure 8. Polysome Loading of mRNAs in the *eif3h* Mutant.

RNA from 10-d-old wild-type and *eif3h-1* mutant seedlings grown on 1% sucrose was fractionated on sucrose gradients. The gradients analyzed in **(C)** to **(E)**, which were run separately from those in **(A)** and **(B)**, were fractionated manually (see Methods). The experiment shown in **(C)** to **(E)** was repeated once, with similar results.

(A) and **(B)** UV absorbance profiles of gradients from the wild type **(A)** and *eif3h-1* **(B)**.

(C) Ethidium bromide–stained RNA gels indicating the distribution of 28S and 18S rRNAs as indicators of 60S large and 40S small ribosomal subunits, respectively. The enrichment of the 60S subunit/ 28S rRNA in fractions 5/6 defines the heavier fractions as monosomes and polysomes.

(D) and **(E)** The level of ATB2 mRNA and rbcS mRNA **(D)** per fraction was examined by RT-PCR. Results in **(D)** are representative of two independent polysome gradients. Likewise, luciferase mRNA, which had been added to each sample after fractionation, was amplified as an internal control **(E)**. In the ATB2 panels, peak fractions are indicated with arrowheads.

complex onto 40S ribosomes (Benne and Hershey, 1978). eIF3 interacts with eIF4G, an event thought to recruit the 43S complex to the cap binding complex. Given the established role of eIF3 in loading the 40S ribosome with the ternary complex, eIF2-GTP-$tRNA^{Met}$, a stimulatory role for eIF3h in reinitiation at an AUG codon downstream of a uORF is an attractive hypothesis. However, eIF3h may also be involved in the fidelity of start codon recognition, in the processing of potentially inhibitory uORF translation products, or in the resumption of ribosome scanning downstream of a uORF (Nielsen et al., 2004; Pöyry et al., 2004; Rajkowitsch et al., 2004). These possibilities remain to be explored in future work.

eIF3 and Development

The notion that noncore subunits of eIF3 are dispensable for global translation is supported by our results, which show that seedlings of the *eif3h-1* mutant incorporated amino acids into protein with a similar efficiency as the wild type (Figure 7A). Differences in the profile of in vivo–labeled protein bands between *eif3h* and the wild type are presumably because of both direct, translational, and indirect, developmental effects. The UV profile of sucrose-fractionated RNA may suggest a reduction in the polysome-to-monosome ratio in the *eif3h* mutant, a result seemingly at odds with the in vivo labeling experiment. Differences in the plant growth conditions may have contributed to this discrepancy, and further experiments are needed to clarify the quantitative extent of global translational defects upon disruption of *eIF3h*. However, when compared with mutants in yeast, the effect of the Arabidopsis *eif3h* mutation is more reminiscent of the subtle effects of the noncore *eIF3e*/*Int6* or *Pci8p* mutations rather than the dramatic defects seen upon loss of the core subunit eIF3b/PRT1 (Akiyoshi et al., 2000; Nielsen et al., 2004).

The developmental consequences of the loss of eIF3h were diverse and included growth retardation, morphological abnormalities, reduced fertility (especially through the male gametophytic lineage), seedling arrest in the absence of an external carbon source, and hypersensitivity to external sugars and the plant hormone ABA. Responses to several other plant hormones were altered as well, including reduced sensitivity to ethylene in darkness and increased sensitivity to brassinosteroids under both light and dark conditions (T.-H. Kim and A.G. von Arnim, unpublished data). Consistent with the morphological defects, which suggested alterations in the auxin response, we observed an elevation of specific AUX/IAA mRNAs. Given that the AUX/IAA mRNAs are not known to be translationally regulated and do not contain uORFs, their elevation may be understood as an indirect consequence of the *eif3h* mutation rather than a stabilization as a result of their direct translational stimulation by eIF3h.

Whether and how the undertranslation of specific mRNAs contributes to the phenotypic spectrum of the *eif3h* mutant remains to be defined. The ATB2 mRNA, for example, is light induced at the transcriptional level, derepressed in darkness in the etiolation deficient mutants *cop1* and *det1*, and translationally repressed by sucrose. Moreover, sucrose in the range of 25 to 50 mM (0.8 to 1.7%) is known to repress photosynthetic gene expression (Rook et al., 1998a, 1998b). It is plausible, but by no means self-evident, that ATB2 may play a role in deetiolation and greening and that the greening defects seen in the presence of sucrose in the *eif3h* mutant (Figure 5A) are a consequence of the misexpression of ATB2. Establishing a cause-and-effect relationship, however, will require future work, especially in light of the fact that ATB2 is a member of a gene family with multiple members under translational control (Martinez-Garcia et al.,

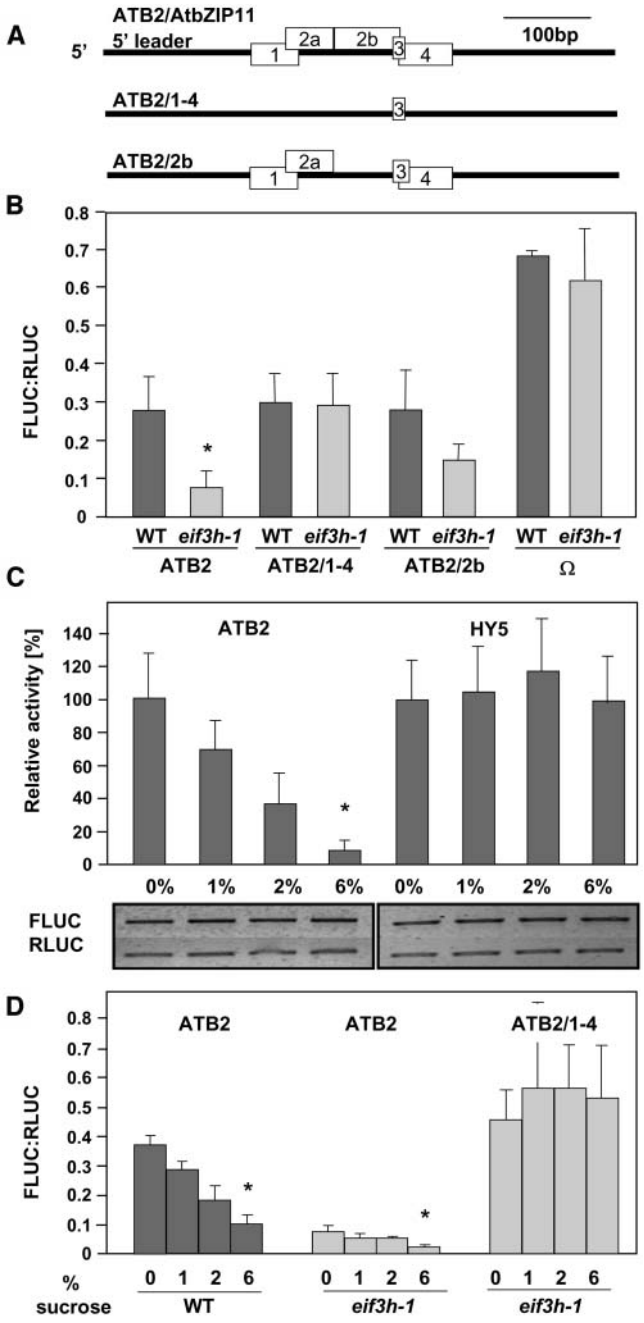

Figure 9. Regulation of Translation by uORFs and Sucrose.

(A) Schematic drawing of the four overlapping uORFs in the ATB2/AtbZIP11 5′ leader sequence.

(B) Translational efficiency was examined for the wild-type ATB2 leader, a mutation eliminating uORFs 1, 2a, 2b, and 4 (ATB2/1-4) and a mutation eliminating the sucrose regulatory uORF 2b (ATB2/2b), as well as the TMV Ω leader as a control. Wild-type and *eif3h* mutant seedlings were grown on 1% sucrose. Bars denote standard deviations. Experiments were done in duplicate with similar results.

(C) Translation using the ATB2 and HY5 leaders was examined in wild-type seedlings grown on the indicated concentrations of sucrose. The mean of the ATB2 data at 0% sucrose was set to 100%. RT-PCR products from corresponding RNA samples are shown below the bar graph.

(D) Wild-type and *eif3h* mutant seedlings were grown on 1% sucrose, transferred to the indicated sucrose condition, cobombarded with the indicated ATB2 expression and TL-RLUC reference construct, and incubated for 48 h before analysis of gene expression.

Asterisks in **(B)** to **(D)** symbolize the results from a Student's *t* test in a pairwise comparison with the corresponding wild-type sample **(B)** or 1% sucrose sample (**[C]** and **[D]**). One asterisk, $P < 0.05$.

1998; Wiese et al., 2004). At the same time, the pleiotropic phenotype of the *eif3h* mutant can be rationalized by postulating that many additional mRNAs other than ATB2 depend on eIF3h for effective translation.

The Interaction between eIF3 and the CSN

Our data confirm and extend previous observations indicating a biochemical interaction between eIF3 and the CSN (Karniol et al., 1998; Yahalom et al., 2001), two structurally related PCI complexes. EIF3h interacted with multiple CSN subunits in yeast two-hybrid assays, and an antibody against eIF3h was able to coimmunoprecipitate the CSN4 and CSN5 subunits. Although the efficiency of coimmunoprecipitation was not high, it should be emphasized that the data were collected from wild-type Arabidopsis extracts with untagged proteins at their native expression levels. The interaction of eIF3h with the CSN may also be tissue specific or otherwise conditional. Mutants in the CSN share certain similarities with the *eif3h* mutant phenotype described here. For example, without sucrose, both mutants arrest their development at the same stage, right after germination, and root growth is stimulated by sucrose (Figures 5A and 6A). Interestingly, the *fus6*/CSN1-11 line, which retains a reduced level of the CSN (Wang et al., 2003b), suffers from growth retardation, floral developmental abnormalities, and fertility defects (Wang et al., 2003b), which are reminiscent of the *eif3h* mutant. The defects in *fus6*/CSN1-11 have not been attributable to the deneddylation activity of the CSN because, other than in *fus6*/*csn1* null mutants, cullins are Nedd8 modified normally in the *fus6*/CSN1-11 line (Wang et al., 2003b). Finally, double mutants between *csn8* and *eif3h* displayed synthetic lethality during embryogenesis, as early as the heart stage (i.e., at a stage when either single mutant was indistinguishable from the wild type). This defect, which was most pronounced in the root-shoot axis, suggests a functional interaction between *eIF3h* and *CSN* genes.

Biochemical interactions between the PCI complexes are also emerging in other organisms. Mammalian eIF3e can interact with CSN subunits (Hoareau Alves et al., 2002). The closest homolog of eIF3e/Int6 in budding yeast, Pci8p, is associated with eIF3 but also functions in the context of a CSN-like complex (Shalev et al., 2001; Wee et al., 2002; Maytal-Kivity et al., 2003). Moreover, eIF3e/Int6 of fission yeast is associated with the third PCI complex, the proteasome lid, and its deletion causes hyperaccumulation of ubiquitinated proteins (Yen et al., 2003). Whereas this mechanistic data set on the eIF3h subunit clearly suggests its involvement in translation (Figures 7 to 9), an interaction between eIF3h and the CSN may help to coordinate

the respective cellular activities of the two complexes in translation initiation and protein turnover, respectively.

METHODS

Growth Conditions and Mutant Isolation

General growth conditions for *Arabidopsis thaliana* were described previously (Stacey et al., 1999). Seedlings were grown on agar plates or in liquid medium containing 1× strength Murashige and Skoog salts, pH 5.7, and 1% sucrose. For auxin treatment, seedlings were grown on agar plates containing 1 μM 2,4-D (Sigma, St. Louis, MO) for 6 d before RNA isolation. The effect of ABA (Sigma) was observed after 6 d of incubation of sterilized Arabidopsis seeds on agar plates containing ABA. For in vivo labeling, seedlings were grown on plates for 7 d and then incubated in liquid 1× MS medium containing Trans [^{35}S] Label (ICN Biomedical, Irvine, CA) at a concentration of 40 μCi/mL for 1 h before harvest. Wild-type plants and the *eif3h* mutant were in the Columbia background. The *csn8*/*cop9*, *csn1*/*fus6*/*cop11*, and *csn7*/*fus5* mutants are described by Wei et al. (1992) (1994) and Karniol et al. (1999), respectively. A T-DNA insertion collection was screened for mutants in *eIF3h* using primers 5′-TTTCACTATCACCGGAGACTATTTCAATG-3′ and 5′-TTGGGTAGT-CTTTGCAATCAGTTGTCGTG-3′ in collaboration with the Arabidopsis Knockout Facility (University of Wisconsin; Sussman et al., 2000). This line was backcrossed twice, without a significant effect on the phenotypes described here. Double mutants between *eif3h-1* and *csn8* were identified in siliques from *eif3h-1* mutant F2 plants that had been scored for the *csn8-1* T-DNA insertion allele by PCR. Embryos were expelled manually from nearly mature seeds.

Molecular Cloning and Protein Analysis

cDNA of eIF3h from the start to the stop codon was amplified (from EST N96519; Burks et al., 2001) by PCR with the primers 5′-GACTAGATC-T**ATG**GCAACCATGGCTAGGTCGTTTC-3′ and 5′-GTCTCTCGAG**TCA**-GTTGTCGTGCAATGCTTTGGTC-3′. The protein coding region was digested with *Bgl*II/*Xho*I and inserted into pET30a (Novagen, Madison, WI) and pGEX4T-1 (Pharmacia, Buckinghamshire, UK) for production of recombinant eIF3h proteins in *Escherichia coli* strain BL21. A rabbit antiserum was raised against His_6-tagged eIF3h (Covance, Berkeley, CA) and then affinity purified against glutathione *S*-transferase–tagged eIF3h protein coupled to a Hi Trap affinity column (Amersham-Pharmacia Biotech, Uppsala, Sweden) as described previously (Yahalom et al., 2001). Other antibodies against eIF3e and eIF3b were from Yahalom et al. (2001). Antibodies against CSN4, CSN5, and ubiquitin were purchased from Affinity-Biomol (Plymouth Meeting, PA).

Total plant protein was extracted in grinding buffer (400 mM sucrose, 10% [w/v] glycerol, 10 mM KCl, 50 mM Tris-HCl, pH 8.0, 10 mM EDTA, and 1× protease inhibitor cocktail; Sigma) and quantified by BCA assays (Pierce, Rockford, IL). Proteins were separated in 10 or 12.5% acrylamide gels by SDS-PAGE and then electroblotted to a polyvinylidene difluoride membrane. Immunoblots were probed with the indicated primary antibody and with alkaline phosphatase labeled secondary antibody and developed using chemiluminescent substrate (Roche, Indianapolis, IN). For gel filtration chromatography, Arabidopsis was ground in liquid nitrogen and suspended in a phosphate buffer, pH 7.0, containing 10% glycerol, 10 mM NaCl, 10 mM $MgCl_2$, 5 mM EDTA, 0.5 mM phenylmethylsulfonyl fluoride, and complete protease inhibitor mixture tablets (Roche). After 30 min of centrifugation at 22,000*g* at 4°C, the supernatant was filtered through a 0.45-μm filter (Sartorius, Göttingen, Germany). Approximately 800 μg of total protein was loaded on a superose 6 HR column (Amersham-Pharmacia Biotech) equilibrated with 50 mM Tris-HCl, pH 7.5, 150 mM NaCl, 10 mM $MgCl_2$, 5 mM EDTA, and 5% glycerol. Fractions were collected and concentrated using Strata Clean resin beads (Stratagene, La Jolla, CA) and analyzed by immunoblotting.

Transgenic Plants and RNA Analysis

For complementation of the *eif3h-1* mutant, the coding region of *eIF3h* was inserted behind 1900 bp of the immediate 5′ upstream region of the *eIF3h* coding region in the binary vector pCAMBIA-1300. Homozygous *eif3h-1* mutant plants were transformed using *Agrobacterium tumefaciens* by the floral dip method, and transformants were selected on MS agar plates containing 30 mg/L of hygromycin.

Total RNA was prepared by grinding tissues in liquid nitrogen and extracting with Trizol (Sigma). For RNA gel blots, equal amounts of RNA were separated by 1% agarose/formaldehyde gel electrophoresis and then transferred to positively charged nylon membranes (Roche). Digoxygenin-labeled or α-^{32}P–labeled probes were prepared using the DNA labeling kit (Roche) or the random prime labeling system (Amersham Biosciences, Piscataway, NJ), respectively. The cDNAs of IAA3 (C00011, At1g04240) and IAA14 (C00046, At4g14550) were provided by the Arabidopsis Biological Resource Center, and IAA17 (At1g04250) was amplified by PCR from genomic DNA. RNA gel blots were hybridized in DIG Easy Hyb (Roche) and washed two times at 65°C with 2× SSC (1× SSC is 0.15 M NaCl and 0.015 M sodium citrate) and 0.1% SDS followed by two washes with 0.1× SSC and 0.1% SDS for 20 min each.

For the RT-PCR assay, 1 μg of total RNA was treated with RNase-free DNase I (Promega, Madison, WI) and used to synthesize cDNAs with a 15-mer oligo(dT) primer using MMLV reverse transcriptase (Promega). The cDNA products served as templates for the subsequent PCR reactions with the condition of 25 cycles for β-tubulin and 30 cycles for other target genes at 95°C for 30 s, 60°C for 30 s, and 72°C for 1min. Primer sequences for the amplification of β-tubulin, ATB2, HY5, RBCS, LHY, FLUC, and RLUC are available upon request.

Polysome Fractionation

Arabidopsis polysomes were fractionated over sucrose gradients as described (Dickey et al., 1998) with minor modifications. Approximately 500 mg of 10-d-old seedlings were ground in liquid nitrogen and then in 1 mL of extraction buffer (0.2 M Tris-HCl, pH 8.0, 50 mM KCl, 25 mM $MgCl_2$, 1% Triton X-100, 400 units/mL of RNasin, and 50 μg/mL of cycloheximide). After spinning for 10 min at 4°C, 800 μL of supernatant was loaded onto a 10-mL 15 to 50% sucrose gradient and spun in a Beckman SW41Ti rotor (Fullerton, CA) at 135000*g* for 3.5 h at 4°C. The UV-absorbance profile was obtained with a gradient fractionator connected to a UA-5 UV absorbance detector (ISCO, Lincoln, NE). Alternatively, 12 0.9-mL fractions were collected manually from the bottom by inserting tubing through the gradient. After extraction with phenol/chloroform/isoamyl alcohol, total RNA was precipitated with isopropanol. Fractionation quality was examined by electrophoresis, and the RNA was treated with DNase I. Two nanograms of FLUC RNA was added as an internal control (Promega), and specific transcripts were amplified by semiquantitative RT-PCR. Independent repeats of the PCR with fewer cycles or additional cycles confirmed that PCR reactions had not reached saturation (data not shown).

Yeast Two-Hybrid and Coimmunoprecipitation Assays

A protein coding region of eIF3a was amplified (from EST W43633; Burks et al., 2001) by PCR with the primers 5′-GTCGGATCC**ATG**GC-GAATTTTGCCAAACCA-3′ and 5′-AACCTCGAGT**CTA**GATGGGCCTG-GAGCTTCCAAAT-3′ (start and stop codons are in bold). LexA DNA binding domain fusions and B42 activation domain fusions for eIF3h, eIF3a, b, and c (Yahalom et al., 2001), as well as for CSN4 and 5, were generated in pEG202 and pJG4-5. Cotransformants of yeast strain

EGY48 (Invitrogen, Carlsbad, CA) containing pSH18-34 were selected. To test for two-hybrid interactions, at least three independent transformants were tested for the expression of the LEU2 and LacZ reporter genes on YNB/galactose/X-Gal plates lacking Leu.

For coimmunoprecipitation, total proteins were extracted from ~0.2 g of 7-d-old seedlings using Co-IP buffer (50 mM Tris-HCl, pH 7.5, 150 mM NaCl, 10 mM $MgCl_2$, 0.2% Nonidet P-40, and 1× protease inhibitor cocktail; Sigma) after grinding in liquid nitrogen. Extracts were cleared by spinning for 10 min at 4°C in a microcentrifuge followed by a second spin of supernatants for 5 min at 4°C. Dimethylpimelidate (40 mM) was used to covalently couple equal amounts of preimmune serum or eIF3h antiserum to protein A-sepharose (Sigma). Approximately 2 mg of total protein extracts in 500 μL of co-IP buffer were incubated with the sepharose-coupled antibody for 4 h at 4°C. Precipitated immunocomplex was washed four times with co-IP buffer and eluted with elution buffer (100 mM Tricine, pH 2.5) and neutralized with one volume of 1 M Tris-HCl, pH 7.5. Neutralized samples were concentrated by ultrafiltration (Millipore, Bedford, MA) and then analyzed by immunoblotting.

Transient Expression and Luciferase Reporter Assays

The wild type and *eif3h* grown for 20 d on MS agar plates containing the indicated sucrose concentration were cotransfected by bombardment (PDS-1000/He; Bio-Rad, Hercules, CA). For the translation assays, various 5′ leader sequences were inserted between the transcription start site of the 35S promoter and a FLUC cDNA. The 5′ leader sequences were derived from the longest cDNA entries in GenBank. The 68 bp of the omega (Ω) motif were synthesized based on published data (Tanguay and Gallie, 1996). The remaining leader sequences included (1) ATB2 (from −540 to +1 as a start codon; At4g34590), (2) CAB2 (from −66 to +37; At1g29930), (3) RBCS (from −35 to +61; At5g38430), (4) HY5 (from −191 to +1; At5g11260), (5) ABI5 (from −167 to +1; At2g36270), and (6) LHY (from −675 to +1, including two introns; At1g01060). CAB2 and RBCS included short sections of the coding sequence. The control plasmid contained a fusion of RLUC to the translational leader of tobacco etch virus (TL; Carrington and Freed, 1990) under the control of the 35S promoter. For eIF3h coexpression experiments, an eIF3h cDNA was amplified with the primers 5′-AGATCCATGGCAACGATGGCTAGG-TCGTTTCTGCAG-3′ and 5′-GTCTCTAGACCATGGTGTCGTGCAATG-CTTTGGTCAG-3′ and cloned between the 35S promoter, TL translational leader, and 35S terminator in the sense orientation. A 35S:YFP plasmid used as a control is described elsewhere (Subramanian et al., 2004). The ATB2/1-4 and ATB2/2b mutated ATB2 leader sequences were kindly provided by Nico Elzinga and Anika Wiese (Wiese et al., 2004) and recloned into the 35S:FLUC expression plasmid. ATB2/1-4 and ATB2/2b are referred to as 5-1.2.4 and 5-2b by Wiese and coworkers. Luciferase activity was measured in protein extracts prepared 20 to 30 h after bombardment using the Dual-Luciferase system (Promega) and the TD-20/20 luminometer (Turner Designs, Sunnyvale, CA). In this system, the two luciferases are distinguished because they use different substrates. Ratios of firefly to RLUC activity were obtained and statistically processed after typically three or four independent experiments to indicate a translational efficiency of the tested 5′ leader sequence.

ACKNOWLEDGMENTS

We thank the University of Wisconsin Arabidopsis Functional Genomics Consortium for T-DNA knockout screening services, the Salk Institute Genomic Analysis Laboratory project for SALK T-DNA insertion mutants, and the Arabidopsis stock center at Ohio State University for cDNAs. We also thank Nico Elzinga, Anika Wiese, Sjef Smeekens, and Hongyong Fu for discussion as well as plasmid constructs. We acknowledge Jonathan Schneiderman for critical technical assistance. Comments from David Brian and Dan Roberts as well as anonymous reviewers on a previous version of the manuscript are also appreciated. A.G.v.A. acknowledges support from the Department of Energy Grant DE-FG02-9620223. D.A.C and A.G.v.A. were supported by Grant 2000320 from the US-Israel Binational Science Foundation and by US-Israel Binational Agricultural Research and Development Grant IS-3451-03.

Received August 12, 2004; accepted September 10, 2004.

REFERENCES

Akiyoshi, Y., Clayton, J., Phan, L., Yamamoto, M., Hinnebusch, A.G., Watanabe, Y., and Asano, K. (2000). Fission yeast homolog of murine Int-6 protein, encoded by mouse mammary tumor virus integration site, is associated with the conserved core subunits of eukaryotic translation initiation factor 3. J. Biol. Chem. **276,** 10056–10062.

Asano, K., Merrick, W.C., and Hershey, J.W.B. (1997a). The translation initiation factor eIF3-p48 subunit is encoded by *int-6*, a site of frequent integration by the mouse mammary tumor virus genome. J. Biol. Chem. **272,** 23477–23480.

Asano, K., Phan, L., Anderson, J., and Hinnebusch, A.G. (1998). Complex formation by all five homologues of mammalian translation initiation factor 3 subunits from yeast *Saccharomyces cerevisiae*. J. Biol. Chem. **273,** 18573–18585.

Asano, K., Vornlocher, H.P., Richter-Cook, N.J., Merrick, W.C., Hinnebusch, A.G., and Hershey, J.W. (1997b). Structure of cDNAs encoding human eukaryotic initiation factor 3 subunits. Possible roles in RNA binding and macromolecular assembly. J. Biol. Chem. **272,** 27042–27052.

Bandyopadhyay, A., Lakshmanan, V., Matsumoto, T., Chang, E.C., and Maitra, U. (2002). Moe1 and spInt6, the fission yeast homologues of mammalian translation initiation factor 3 subunits p66 (eIF3d) and p48 (eIF3e), respectively, are required for stable association of eIF3 subunits. J. Biol. Chem. **277,** 2360–2367.

Bandyopadhyay, A., Matsumoto, T., and Maitra, U. (2000). Fission yeast Int6 is not essential for global translation initiation, but deletion of int6(+) causes hypersensitivity to caffeine and affects spore formation. Mol. Biol. Cell **11,** 4005–4018.

Bech-Otschir, D., Kraft, R., Huang, X., Henklein, P., Kapelari, B., Pollmann, C., and Dubiel, W. (2001). COP9 signalosome-specific phosphorylation targets p53 to degradation by the ubiquitin system. EMBO J. **20,** 1630–1639.

Benne, R., and Hershey, J.W. (1978). The mechanism of action of protein synthesis initiation factors from rabbit reticulocytes. J. Biol. Chem. **253,** 3078–3087.

Burks, E.A., Bezerra, P.P., Le, H., Gallie, D.R., and Browning, K.S. (2001). Plant initiation factor 3 subunit composition resembles mammalian initiation factor 3 and has a novel subunit. J. Biol. Chem. **276,** 2122–2131.

Carrington, J.C., and Freed, D.D. (1990). Cap-independent enhancement of translation by a plant potyvirus 5′ nontranslated region. J. Virol. **64,** 1590–1597.

Castle, L.A., and Meinke, D.W. (1994). A FUSCA gene of Arabidopsis encodes a novel protein essential for plant development. Plant Cell **6,** 25–41.

Chamovitz, D.A., Wei, N., Osterlund, M.T., von Arnim, A.G., Staub, J.M., Matsui, M., and Deng, X.W. (1996). The COP9 complex, a novel

multisubunit nuclear regulator involved in light control of a plant developmental switch. Cell **86,** 115–121.

Cope, G.A., Suh, G.S., Aravind, L., Schwarz, S.E., Zipursky, S.L., Koonin, E.V., and Deshaies, R.J. (2002). Role of predicted metalloprotease motif of Jab1/Csn5 in cleavage of Nedd8 from Cul1. Science **298,** 608–611.

Crane, R., Craig, R., Murray, R., Dunand-Sauthier, I., Humphrey, T., and Norbury, C. (2000). A fission yeast homolog of Int-6, the mammalian oncoprotein and eIF3 subunit, induces drug resistance when overexpressed. Mol. Biol. Cell **11,** 3993–4003.

Dean, K.A., Aggarwal, A.K., and Wharton, R.P. (2002). Translational repressors in Drosophila. Trends Genet. **18,** 572–577.

Dickey, L.F., Petracek, M.E., Nguyen, T.T., Hansen, E.R., and Thompson, W.F. (1998). Light regulation of Fed-1 mRNA requires an element in the 5′ untranslated region and correlates with differential polyribosome association. Plant Cell **10,** 475–484.

Gallie, D.R., Le, H., Tanguay, R.L., and Browning, K.S. (1998). Translation initiation factors are differentially regulated in cereals during development and following heat shock. Plant J. **14,** 715–722.

Guo, J., Hui, D.J., Merrick, W.C., and Sen, G.C. (2000). A new pathway of translational regulation mediated by eukaryotic initiation factor 3. EMBO J. **19,** 6891–6899.

Hershey, J.W.B., and Merrick, W.C. (2000). The pathway and mechanism of initiation of protein synthesis. In Translational Control of Gene Expression, N. Sonenberg, J.W.B. Hershey, and M. Mathews, eds (Cold Spring Harbor, NY: Cold Spring Harbor Laboratory Press), pp. 33–88.

Hinnebusch, A.G., and Natarajan, K. (2002). Gcn4p, a master regulator of gene expression, is controlled at multiple levels by diverse signals of starvation and stress. Eukaryot. Cell **1,** 22–32.

Hoareau Alves, K., Bochard, V., Rety, S., and Jalinot, P. (2002). Association of the mammalian proto-oncoprotein Int-6 with the three protein complexes eIF3, COP9 signalosome and 26S proteasome. FEBS Lett. **527,** 15–21.

Hofmann, K., and Bucher, P. (1998). The PCI domain: A common theme in three multiprotein complexes. Trends Biochem. Sci. **23,** 204–205.

Holm, M., Ma, L.G., Qu, L.J., and Deng, X.W. (2002). Two interacting bZIP proteins are direct targets of COP1-mediated control of light-dependent gene expression in Arabidopsis. Genes Dev. **16,** 1247–1259.

Hui, D.J., Bhasker, C.R., Merrick, W.C., and Sen, G.C. (2003). Viral stress-inducible protein p56 inhibits translation by blocking the interaction of eIF3 with the ternary complex eIF22GTP2Met-tRNAi. J. Biol. Chem. **278,** 39477–39482.

Karniol, B., Yahalom, A., Kwok, S., Tsuge, T., Matsui, M., Deng, X.W., and Chamovitz, D.A. (1998). The Arabidopsis homologue of an eIF3 complex subunit associates with the COP9 complex. FEBS Lett. **439,** 173–179.

Kawaguchi, R., and Bailey-Serres, J. (2002). Regulation of translational initiation in plants. Curr. Opin. Plant Biol. **5,** 460–465.

Kim, J.Y., Song, H.R., Taylor, B.L., and Carré, I.A. (2003). Light-regulated translation mediates gated induction of the Arabidopsis clock protein LHY. EMBO J. **22,** 935–944.

Kim, T., Hofmann, K., von Arnim, A.G., and Chamovitz, D.A. (2001). PCI complexes: Pretty complex interactions in diverse signaling pathways. Trends Plant Sci. **6,** 379–386.

Kim, T.H., Kim, B.H., and von Arnim, A.G. (2002). Repressors of photomorphogenesis. Int. Rev. Cytol. **220,** 185–223.

Koyanagi-Katsuta, R., Akimitsu, N., Hamamoto, H., Arimitsu, N., Hatano, T., and Sekimizu, K. (2002). Embryonic lethality of mutant mice deficient in the p116 gene. J. Biochem. **131,** 833–837.

Leon, P., and Sheen, J. (2003). Sugar and hormone connections. Trends Plant Sci. **8,** 110–116.

Lohmer, S., Maddaloni, M., Motto, M., Salamini, F., and Thompson, R.D. (1993). Translation of the mRNA of the maize transcriptional activator Opaque-2 is inhibited by upstream open reading frames present in the leader sequence. Plant Cell **5,** 65–73.

Lopez-Molina, L., Mongrand, S., and Chua, N.H. (2001). A postgermination developmental arrest checkpoint is mediated by abscisic acid and requires the ABI5 transcription factor in Arabidopsis. Proc. Natl. Acad. Sci. USA **98,** 4782–4787.

Lyapina, S., Cope, G., Shevchenko, A., Serino, G., Tsuge, T., Zhou, C., Wolf, D.A., Wei, N., and Deshaies, R.J. (2001). Promotion of NEDD-CUL1 conjugate cleavage by COP9 signalosome. Science **292,** 1382–1385.

Martinez-Garcia, J.F., Moyano, E., Alcocer, M.J., and Martin, C. (1998). Two bZIP proteins from Antirrhinum flowers preferentially bind a hybrid C-box/G-box motif and help to define a new sub-family of bZIP transcription factors. Plant J. **13,** 489–505.

Matsumoto, S., Bandyopadhyay, A., Kwiatkowski, D.J., Maitra, U., and Matsumoto, T. (2002). Role of the Tsc1-Tsc2 complex in signaling and transport across the cell membrane in the fission yeast *Schizosaccharomyces pombe*. Genetics **161,** 1053–1063.

Mayeur, G.L., and Hershey, J.W. (2002). Malignant transformation by the eukaryotic translation initiation factor 3 subunit p48 (eIF3e). FEBS Lett. **514,** 49–54.

Maytal-Kivity, V., Pick, E., Piran, R., Hofmann, K., and Glickman, M.H. (2003). The COP9 signalosome-like complex in *S. cerevisiae* and links to other PCI complexes. Int. J. Biochem. Cell Biol. **35,** 706–715.

Maytal-Kivity, V., Reis, N., Hofmann, K., and Glickman, M.H. (2002). MPN+, a putative catalytic motif found in a subset of MPN domain proteins from eukaryotes and prokaryotes, is critical for Rpn11 function. BMC Biochem. **3,** 28.

Mundt, K.E., Liu, C., and Carr, A.M. (2002). Deletion mutants in COP9/signalosome subunits in fission yeast *Schizosaccharomyces pombe* display distinct phenotypes. Mol. Biol. Cell **13,** 493–502.

Nielsen, K.H., Szamecz, B., Valasek, L., Jivotovskaya, A., Shin, B.S., and Hinnebusch, A.G. (2004). Functions of eIF3 downstream of 48S assembly impact AUG recognition and GCN4 translational control. EMBO J. **23,** 1166–1177.

Osterlund, M.T., Hardtke, C.S., Wei, N., and Deng, X.W. (2000). Targeted destabilization of HY5 during light-regulated development of Arabidopsis. Nature **405,** 462–466.

Park, H.S., Browning, K.S., Hohn, T., and Ryabova, L.A. (2004). Eucaryotic initiation factor 4B controls eIF3-mediated ribosomal entry of viral reinitiation factor. EMBO J. **23,** 1381–1391.

Park, H.S., Himmelbach, A., Browning, K.S., Hohn, T., and Ryabova, L.A. (2001). A plant viral ''reinitiation'' factor interacts with the host translational machinery. Cell **106,** 723–733.

Pestova, T.V., Kolupaeva, V.G., Lomakin, I.B., Pilipenko, E.V., Shatsky, I.N., Agol, V.I., and Hellen, C.U. (2001). Molecular mechanisms of translation initiation in eukaryotes. Proc. Natl. Acad. Sci. USA **98,** 7029–7036.

Poyry, T.A., Kaminski, A., and Jackson, R.J. (2004). What determines whether mammalian ribosomes resume scanning after translation of a short upstream open reading frame? Genes Dev. **18,** 62–75.

Rajkowitsch, L., Vilela, C., Berthelot, K., Ramirez, C.V., and McCarthy, J.E. (2004). Reinitiation and recycling are distinct processes occurring downstream of translation termination in yeast. J. Mol. Biol. **335,** 71–85.

Rasmussen, S.B., Kordon, E., Callahan, R., and Smith, G.H. (2001). Evidence for the transforming activity of a truncated Int6 gene, in vitro. Oncogene **20,** 5291–5301.

Rook, F., and Bevan, M.W. (2003). Genetic approaches to understanding sugar-response pathways. J. Exp. Bot. **54,** 495–501.

Rook, F., Gerrits, N., Kortstee, A., van Kampen, M., Borrias, M., Weisbeek, P., and Smeekens, S. (1998b). Sucrose-specific signalling represses translation of the Arabidopsis ATB2 bZIP transcription factor gene. Plant J. **15,** 253–263.

Rook, F., Weisbeek, P., and Smeekens, S. (1998a). The light-regulated Arabidopsis bZIP transcription factor gene ATB2 encodes a protein with an unusually long leucine zipper domain. Plant Mol. Biol. **37,** 171–178.

Saramaki, O., Willi, N., Bratt, O., Gasser, T.C., Koivisto, P., Nupponen, N.N., Bubendorf, L., and Visakorpi, T. (2001). Amplification of EIF3S3 gene is associated with advanced stage in prostate cancer. Am. J. Pathol. **159,** 2089–2094.

Schaffer, R., Ramsay, N., Samach, A., Corden, S., Putterill, J., Carré, I.A., and Coupland, G. (1998). The late elongated hypocotyl mutation of Arabidopsis disrupts circadian rhythms and the photoperiodic control of flowering. Cell **93,** 1219–1229.

Schwechheimer, C., Serino, G., Callis, J., Crosby, W.L., Lyapina, S., Deshaies, R.J., Gray, W.M., Estelle, M., and Deng, X.W. (2001). Interactions of the COP9 signalosome with the E3 ubiquitin ligase SCFTIRI in mediating auxin response. Science **292,** 1379–1382.

Serino, G., Su, H., Peng, Z., Tsuge, T., Wei, N., Gu, H., and Deng, X.W. (2003). Characterization of the last subunit of the Arabidopsis COP9 signalosome: Implications for the overall structure and origin of the complex. Plant Cell **15,** 719–731.

Shalev, A., Valasek, L., Pise-Masison, C.A., Radonovich, M., Phan, L., Clayton, J., He, H., Brady, J.N., Hinnebusch, A.G., and Asano, K. (2001). *Saccharomyces cerevisiae* protein Pci8p and human protein eIF3e/Int-6 interact with the eIF3 core complex by binding to cognate eIF3b subunits. J. Biol. Chem. **276,** 34948–34957.

Stacey, M.G., Hicks, S.N., and von Arnim, A.G. (1999). Discrete domains mediate the light-responsive nuclear and cytoplasmic localization of Arabidopsis COP1. Plant Cell **11,** 349–364.

Subramanian, C., Kim, B.H., Lyssenko, N.N., Xu, X., Johnson, C.H., and von Arnim, A.G. (2004). The Arabidopsis repressor of light signaling, COP1, is regulated by nuclear exclusion: Mutational analysis by bioluminescence resonance energy transfer. Proc. Natl. Acad. Sci. USA **101,** 6798–6802.

Sussman, M.R., Amasino, R.M., Young, J.C., Krysan, P.J., and Austin-Phillips, S. (2000). The Arabidopsis knockout facility at the University of Wisconsin-Madison. Plant Physiol. **124,** 1465–1467.

Tanguay, R.L., and Gallie, D.R. (1996). Isolation and characterization of the 102-kilodalton RNA-binding protein that binds to the 5′ and 3′ translational enhancers of tobacco mosaic virus RNA. J. Biol. Chem. **271,** 14316–14322.

Uhle, S., Medalia, O., Waldron, R., Dumdey, R., Henklein, P., Bech-Otschir, D., Huang, X., Berse, M., Sperling, J., Schade, R., and Dubiel, W. (2003). Protein kinase CK2 and protein kinase D are associated with the COP9 signalosome. EMBO J. **22,** 1302–1312.

Valasek, L., Nielsen, K.H., and Hinnebusch, A.G. (2002). Direct eIF2-eIF3 contact in the multifactor complex is important for translation initiation in vivo. EMBO J. **21,** 5886–5898.

Verma, R., Aravind, L., Oania, R., McDonald, W.H., Yates III, J.R., Koonin, E.V., and Deshaies, R.J. (2002). Role of Rpn11 metalloprotease in deubiquitination and degradation by the 26S proteasome. Science **298,** 611–615.

Wang, C., Pflugheber, J., Sumpter, R., Jr., Sodora, D.L., Hui, D., Sen, G.C., and Gale, M., Jr. (2003a). Alpha interferon induces distinct translational control programs to suppress hepatitis C virus RNA replication. J. Virol. **77,** 3898–3912.

Wang, L., and Wessler, S.R. (1998). Inefficient reinitiation is responsible for upstream open reading frame-mediated translational repression of the maize R gene. Plant Cell **10,** 1733–1746.

Wang, X., Feng, S., Nakayama, N., Crosby, W.L., Irish, V., Deng, X.W., and Wei, N. (2003b). The COP9 signalosome interacts with SCFUFO and participates in Arabidopsis flower development. Plant Cell **15,** 1071–1082.

Wee, S., Hetfeld, B., Dubiel, W., and Wolf, D.A. (2002). Conservation of the COP9/signalosome in budding yeast. BMC Genet. **3,** 15.

Wei, N., and Deng, X.W. (1999). Making sense of the COP9 signalosome. A regulatory protein complex conserved from Arabidopsis to human. Trends Genet. **15,** 98–103.

Wei, N., and Deng, X.W. (2003). The COP9 signalosome. Annu. Rev. Cell Dev. Biol. **19,** 261–285.

Wiese, A., Elzinga, N., Wobbes, B., and Smeekens, S. (2004). A conserved upstream open reading frame mediates sucrose-induced repression of translation. Plant Cell **16,** 1717–1729.

Yahalom, A., Kim, T.H., Winter, E., Karniol, B., von Arnim, A.G., and Chamovitz, D.A. (2001). Arabidopsis eIF3e (INT-6) associates with both eIF3c and the COP9 signalosome subunit CSN7. J. Biol. Chem. **276,** 334–340.

Yen, H.C., and Chang, E.C. (2000). Yin6, a fission yeast Int6 homolog, complexes with Moe1 and plays a role in chromosome segregation. Proc. Natl. Acad. Sci. USA **97,** 14370–14375.

Yen, H.C., Gordon, C., and Chang, E.C. (2003). *Schizosaccharomyces pombe* Int6 and Ras homologs regulate cell division and mitotic fidelity via the proteasome. Cell **112,** 207–217.

Zhang, J., and Maquat, L.E. (1997). Evidence that translation reinitiation abrogates nonsense-mediated mRNA decay in mammalian cells. EMBO J. **16,** 826–833.

Zhou, C., Wee, S., Rhee, E., Naumann, M., Dubiel, W., and Wolf, D.A. (2003). Fission yeast COP9/signalosome suppresses cullin activity through recruitment of the deubiquitylating enzyme Ubp12p. Mol. Cell **11,** 927–938.